Powder Technology 356 (2019) 222–230

Contents lists available at ScienceDirect

Powder Technology

journal homepage: www.elsevier.com/locate/powtec

Experiments and CFD-DEM simulations of cohesive particles sedimentation in stilled fluid

Runrun Lu [a], Lin Zhang [a], Philippe Ricoux [b], Limin Wang [a,*]

[a] State Key Laboratory of Multiphase Complex Systems, Institute of Process Engineering, Chinese Academy of Sciences, Beijing 100190, China
[b] Data Processing and Modeling, TOTAL Scientific Division, 24, cours Michelet LA DEFENSE 10, 92069 Paris La Defense CEDEX, France

ARTICLE INFO

Article history:
Received 11 September 2018
Received in revised form 4 February 2019
Accepted 9 May 2019
Available online 11 May 2019

Keywords:
Cohesive force
CED-DEM
Coefficient quantization
Correlation method

ABSTRACT

Particle agglomeration is observed in slurry loop reactors due to the presence of cohesive force between the swollen polyethylene (PE) particles, which has direct impact on the hydrodynamics predictions. However, a qualitative study of the cohesive forces in the suspensions of swollen PE particle at the microscopic level is still lacking. In this study, a simulation contrast experiment method for quantification of cohesive force is proposed. The simulation method is based on a coupled computational fluid dynamics and discrete element method (CFD-DEM) approach, which have been used to study and explain the effects of cohesion on fluidization of particles. The DEM allows the dynamic simulation of the solid phase motion by tracking individual particles, whereas a CFD algorithm is commonly used to simulate the flow field of the continuous fluid phase. The swollen PE particles, initially arranged within a cylinder region in a quiescent hot dodecane, are made to fall, and their sedimentation induces the liquid flow around them. The interactions between the particle motion and the liquid flow are favorably compared with the experimental data, demonstrating the value of the cohesive energy density for the swollen PE particles is between 4000 J/m^3 and 5000 J/m^3.

1. Introduction

Polyethylene (PE) is one of the most essential polymers among the commodity thermoplastic materials, and it has been widely studied so far. Especially, the PE particles are finding an ever-increasing number of applications in nanotechnology, quantum electronics, optoelectronic, coatings, biomedical and information technology. However, as far as the PE particles are concerned, one problem is the occurrence of agglomeration at high temperatures when they are swollen. In this phenomenon, the PE particles will adhere to each other and form larger agglomerates due to the presence of cohesive force. Therefore, it is very important to gain a better understanding for cohesive force between swollen PE particles.

Cohesive forces arise from a variety of sources including liquid bridges, solid bridges, van der Waals forces, electrostatic forces and magnetic forces. In order to quantify the cohesive interaction, a lot of experimental techniques have been developed. For example, a video-contact angles measuring device [1] can perform the cohesive process by measuring contact material surface energy. Destructive and non-destructive cohesive tests [2] are employed to characterize the contact joint cohesive strength. Pull-off force measurements using atomic force microscope (AFM) [3] represent the most common method to characterize and quantify the cohesive force experimentally. At the same time, many cohesive models have also been proposed, mainly including Johnson-Kendall-Roberts (JKR) [4], the Derjaguin-Muller-Toporov (DMT) [5] and van der Walls models [6]. The JKR model considers the surface force acting over the contact area, causing deformation at the contact point. In contrast, the DMT model considers attractive force effects within the ring-shaped zone just outside the contact area. Both the JKR and DMT models have been shown to be the limiting cases of the more general Muller-Yushchenko-Derjaguin (MYD) model [7]. The van der Waals force is the most basic interaction force between particles within the distance at 100 nm, which is the sum of the interaction between atoms or molecules of particles. For fine and ultrafine particles systems, cohesive forces of van der Waals type are commonly considered in the fluidization/defluidization and the van der Walls force between two equal-sized, spherical fine and ultrafine particles is estimated by Hamaker model [6].

The effect of van der Waals force is insignificant and solid bridging and liquid bridging are the sources of cohesion in this study due to the swollen PE particle diameter of 0.5 mm (classified as a Geldart group B particle) is used. Thus here a simplified Johnson-Kendall-Roberts model (SJKR for short) is employed as a simple and representative form of the cohesive forces to characterize the cohesive interaction between swollen PE particles. However, the SJKR model faces some disadvantages, which seriously influence its application in practice. Specially, the coefficient of the SJKR model is hard to determined, leading to that

* Corresponding author.
E-mail addresses: lmwang@ipe.ac.cn, multiphase@hotmail.com (L. Wang).

https://doi.org/10.1016/j.powtec.2019.05.018
0032-5910/

the measuring accuracy of the cohesive force is not high. Aiming at this shortcoming of the SJKR model, in this paper a technique to measure the cohesive force between swollen PE particles is developed. That is to say, the coefficient of cohesive force will be measured, and it will be determined by comparing the CFD-DEM simulation results for swollen PE particles settling in still fluid with a corresponding experiment.

With rapid development of computer science and numerical simulation, discrete particle simulation, a combined computational fluid dynamics (CFD) and discrete element method (DEM) approach, has become one of the most important methods in the field of computational fluidization and multiphase flow [8–10]. CFD-DEM is a typical Euler-Lagrange model, its consists of two parts: the Eulerian part (CFD) for the local liquid (or gas) density and velocity, and the Lagrangian part (DEM) for the position and velocity of each individual solid particle [11], DEM, originates from the late seventies with the original paper of Cundall and Strack [12], can capture interactions between solid particles at the scale of the particle [13], thus giving the opportunity to both track the motion of each particle and examine the granular flow and packing as a whole. In the present work, the particle-fluid forces in the CFD-DEM model included the drag force, pressure gradient force and viscous force, where the drag force is based on the correlation formulated by Di Felice [14].

The rest of the paper is organized as follows: Section 2 presents basic parameters setting in simulation for numerical methods (CFD-DEM) and introduces the cohesive model (SJKR) used in DEM. The third section is about experiment on particles sedimentation at different temperatures. The experiments use the high performance video camera to capture the morphology of particles. In the last section, we will use the correlation method to determine the coefficient *k*.

2. Numerical methods and basic parameters

2.1. The parameter setting for CFD-DEM simulations

In the CFD–DEM simulations, we should define the boundary conditions firstly. At the inlet, the pressure is specified as the atmospheric pressure, and the other walls are no-slip walls for the liquid-phase. We perform simulations of liquid-fluidization of three temperatures (75 °C, 80 °C, 85 °C) in a 3D rectangular fluidized bed. It is found that when the temperature is greater than 70 °C, the particle swelling rapidly and when the temperature is greater than or equal to 90 °C, the particles are dissolved, so we chose the three temperatures above. Table 1 depicts these computational domains. 1 mm × 1 mm structured mesh was employed giving 720,000 number of grids in 3D geometry. At the initial time $t = 0$, spherical solid particles are arranged within a cylinder region of diameter $D = H = 0.01$ m in a quiescent liquid, as shown in Fig. 1, the number of particles is about 6,000. The diameter and density of the particles vary with the ambient temperature. By measuring the expansion ratio and mass change of the particles, the diameter and density of the particle at different temperatures are determined. According to the experimental results, the diameter of the particles increases with the increase of temperature, while the density of the particles changes in the opposite direction. The density of the fluid varies with temperature. The details of simulation parameters are given in Table 1. It is worth noting that in this simulation, the difference between the density of the swelling particles and the density of the fluid is small, it is different from the gas-solid system [15], therefore, the particle

Table 1
Summary of the parameters used in the discrete particle simulation.

Temperature	75 °C	80 °C	85 °C
Liquid phase (Dodecane)			
Density, ρ_l, kg/m^3	708	704	700
Kinematic viscosity, mPa·s	0.645	0.618	0.591
Liquid phase time step, s	5×10^{-4}	5×10^{-4}	5×10^{-4}
Solid phase (PE)			
Diameter, μm	510	520	530
Density, ρ_d, kg/m^3	867	859	853
Particle dynamics time step, s	5×10^{-6}	5×10^{-6}	5×10^{-6}
Bed geometry			
Domain height, m	0.2	0.2	0.2
Domain width, m	0.06	0.06	0.06
Domain depth, m	0.06	0.06	0.06
Number of grid cells	200 × 60 × 60	200 × 60 × 60	200 × 60 × 60

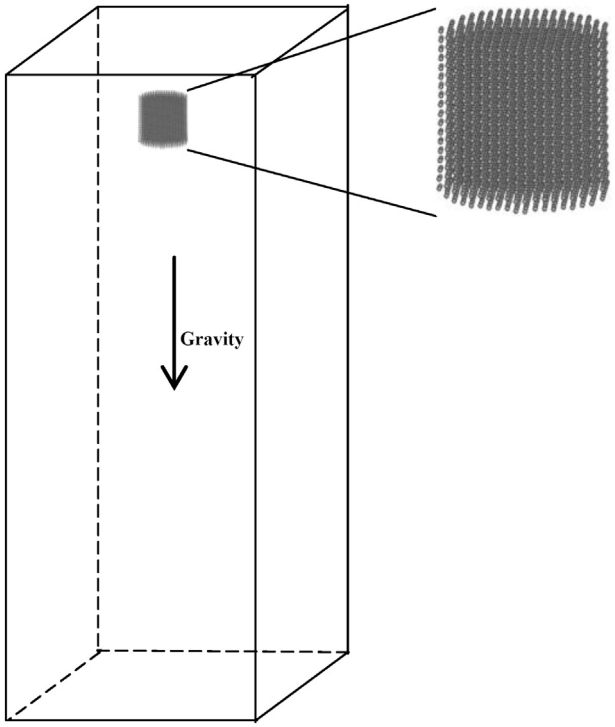

Fig. 1. Simulation domain.

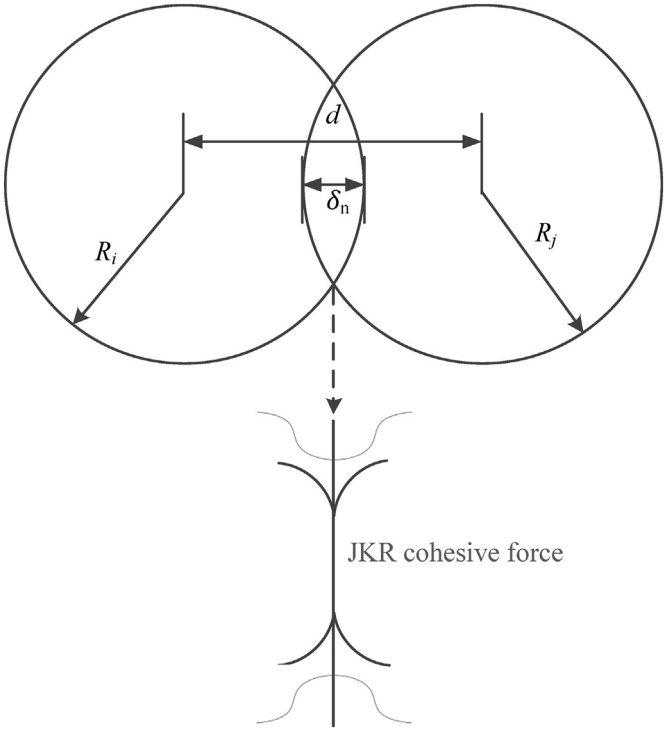

Fig. 2. Schematic of two particles in contact.

Table 2
Experimental apparatus and the related functions.

Apparatus	Functions and the related parameters
Square-type transparent device	Material: glass Size: 0.06m × 0.06m × 0.2m
High-speed camera	Capture the instantaneous shape of the blob when it falls
Constant temperature cabinet	Heat the liquid
Electronic temperature recorder	Measure the temperature of liquid
Sampler	Form the blob of swollen PE particles in cylinder and launch it into liquid slowly

sedimentation velocity may be small, and may reach a nearly uniform settlement state. The physical time is 5 s, because the particle phase and fluid phase coupling will reduce the operation speed, and the fluid phase change is not violent, so run the particle phase one hundred steps, and then coupled with fluid phase.

At the beginning of each simulation, a fixed volume of particles are randomly generated within the cylinder region mentioned in Fig. 1. The particles are allowed to settle due to gravity. It should be emphasized that the height of the simulated area is the same as that of the liquid height in the experiment, also listed in Table 1.

2.2. Simplified Johnson-Kendall-Roberts cohesive model

The JKR model is one of most popular mathematical models which has been used widely in studies. It is well known that the cohesive forces increase with increasing contact area, but it is important to recognize that when two surfaces are in contact (See Fig. 2), it is the asperities on the surface that are in real contact [4]. Johnson, Kendall and Roberts postulate that the cohesive force between two particles is determined by its intrinsic cohesiveness α and the effective contact surface area a:

$$F = \alpha \cdot a \tag{1}$$

where the intrinsic cohesiveness α is defined as the cohesive force exhibited on a unit effective surface area.

For the JKR model which are limited to the spheres with smooth surfaces, without considering the rough surface [16], Hertzian theory predicts the contact radius a_0 is:

$$a_0 = \sqrt[3]{\frac{9}{4}\pi\gamma R^2(1-\upsilon^2)E} \tag{2}$$

The interaction between spheres of the same physical properties to obtain α in JKR model is applied to (i.e. k in SJKR model).

$$\alpha = \frac{3\pi R\gamma}{\pi a_0^2} \tag{3}$$

Substituting $a_0$with Eq. (3) into above expression gives the cohesiveness as follows:

$$\alpha = \frac{1}{\sqrt[3]{\frac{3}{16}\pi^2 R(1-\nu^2)^2/E^2}}\gamma^{\frac{1}{3}} \tag{4}$$

The cohesive model used in this project is a simplified Johnson-Kendall-Roberts (JKR) model. If two particles are in contact, it adds an additional normal force tending to maintain the contact. The form of SJKR model in LIGGGHTS [17] is

$$F = k \cdot A \tag{5}$$

where A denotes the particle contact area and k denotes the cohesive energy density in J/m^3. Different formulations to calculate particle contact area A are available [18]. So for $F = k \cdot A$ in SJKR model, we have

$$k = \alpha \text{ and } A = a \tag{6}$$

For example, in model named SJKR2,

$$A = 2\pi\delta_n \cdot (2R^*) \tag{7}$$

where $\delta_n = d - (R_i + R_j)$ the overlap distance of 2 particles and $\frac{1}{R^*} = \frac{1}{R_i} + \frac{1}{R_j}$. Now the question is to obtain the expression for calculating k.

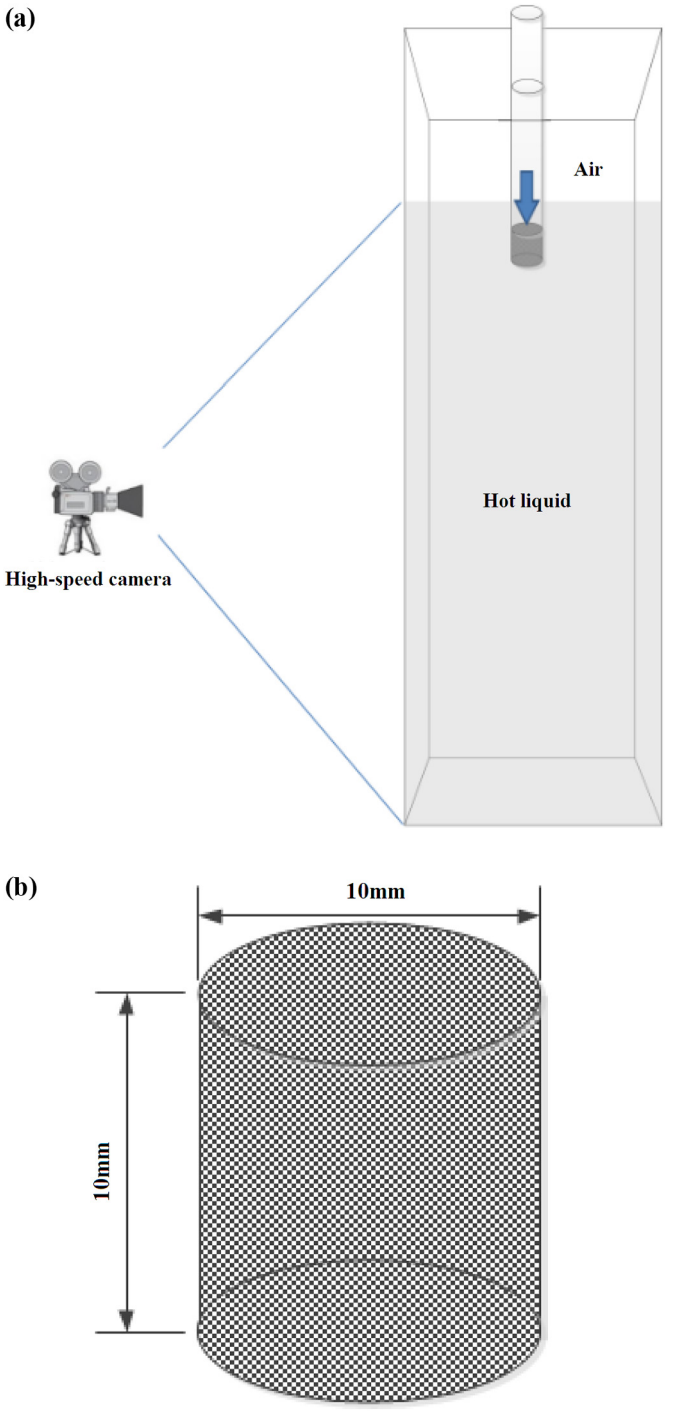

Fig. 3. The schematic diagram of (a) the designed experiment and (b) the size of blob consisted of swollen PE particles.

3. Experiment setup and procedure

3.1. Experiment apparatus

The experiments were conducted by releasing a finite volume of swollen PE particles instantaneously into stagnant hot dodecane (See Table 2). The fluidized bed apparatus is illustrated in Fig. 3. The main parts is a 250 mm high and 60 mm wide-rectangular glass bed. It is vertically placed on the experimental platform. The hot dodecane is poured in and hold temperature. The static height of the liquid is 200 mm. The sampler, which consists of a plastic cylinder of 10 mm diameter, was designed to form the blob of swollen PE particles and launch it into the fluidized bed. The motion of the particles under liquid surface was illuminated by a spotlight and recorded using a video camera (Sony PMW-EX1R) with a resolution of 1920 × 1080 pixels at 25 frames s^{-1}. The background was a white fluorescent lamp, and the particles appeared white and clear in the recorded images. Similar methods have been used in previous literature [19].

Dry particles with a median diameter of $d = 500$ μm and a density of $\rho_s = 870$ g cm^{-3} were swollen. In the swelling process, the diameter increases, while the density decreases, the temperature of the swelling process is different, and the physical properties of the swelling particles are also different. This experiment explored three temperatures, 75 °C, 80 °C and 85 °C, respectively. Before the experiments, the diameter and density of the particles at various temperatures have been measured. Particles in the experiment were carefully placed in a cylindrical container, the height and diameter are both 10 mm, as shown in Fig. 3. The specific parameters, experimental apparatus and the related functions are listed in Table 1.

Fig. 4. Experimental apparatus for measurement of particle sedimentation velocity.

3.2. Experiment procedure

3.2.1. Measurement of time evolution for particle distribution

The dry particles were first swollen in hot dodecane, the particles were swollen respectively at different temperatures, this process was about ten minutes. Then, put swollen PE particles in the bottom of sampler (see Fig. 3) and set up the sampler in the top of square-type transparent device. Inside the square-type transparent device, the hot liquid is poured until the bottom of sampler is submerged (the whole blob is below the level of hot liquid) and the left domain is full of air. Once the liquid becomes stationary and its temperature is at the temperature we want, under the action of cohesive force, swollen PE particles will agglomerate together to form a blob (i.e. the black cylinder in Fig. 3). When to settle down in the liquid, the blob will be deformed and even dispersed due to the action of entrainment exerted on swollen PE particles by liquid, and the original shape of the blob changes, we use high-speed camera to record the related snapshot during the evolution of experiment.

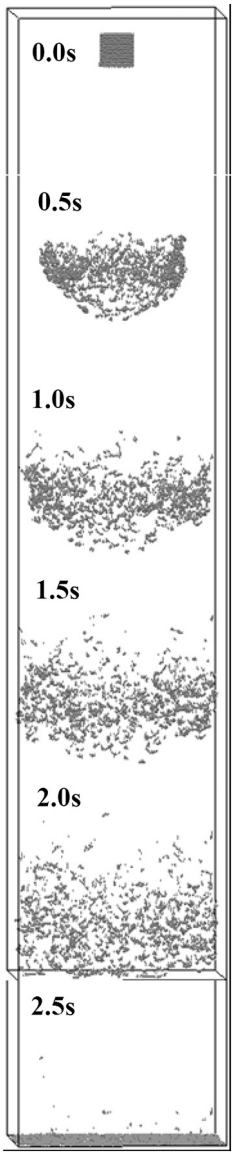

Fig. 5. Time evolution for particle distribution of $k = 4000$ J/m^3 at 85 °C projected onto the verticle plane.

3.2.2. Measurement of particle sedimentation velocity

The velocity-displacement formula is used to measure the velocity of the particles

$$v = s/t \tag{7}$$

Among them, s is the particle sedimentation height. Due to the diffusion of blob in the fall, we measure the velocity of particle which in the front of blob, the device for measuring the drop height is shown in Fig. 4.

Particle fall time is relatively short, so the time interval of the drop height record is 5 frames, that is, 0.2 s.

4. Quantitative and qualitative analysis of the results

4.1. Time evolution of particle distribution and liquid velocity

Particles sedimentation is a process of radial diffusion and axial sedimentation coexist. We choose one of the results as an example. Fig. 5 shows the time evolution for the particle distribution of the situation $k = 4000$ J/m^3 at 85 °C. The particle positions at six time points are projected onto a vertical plane (x–z plane). At the beginning of the sedimentation process, the particles aggregate together in a cylindrical shape and settle under the surface of the liquid. The particles fall with destroying their initial arrangement, namely they tend to disperse in the horizontal direction. This phenomenon is in agreement with the experimental phenomena of Walther [18]. The time evolution for the particle distribution projected onto a horizontal plane (x–y plane) is shown in Fig. 6, where the distributions at the same instance as Fig. 5 are plotted. Though the particles fall with dispersing in the horizontal direction, they distribute within a circular region.

The k is a very important parameter in the SJKR model, and the change of k value directly affects the value of the cohesive force, and then influences the interaction between the liquid and solid. Fig. 7 shows the time evolution for the particle distribution of three k values, 4000 J/m^3, 5000 J/m^3 and 6000 J/m^3, projected onto the verticle plane at 85 °C. From Fig. 7, we can draw the conclusion that was accompanied by an increase in the value of k, the cohesive force between particles increases, and inter-particle cohesion phenomenon is more obvious, the size of the particle aggregation formed by cohesive force is larger, this phenomenon is also reflected in the horizontal direction. Fig. 8 shows

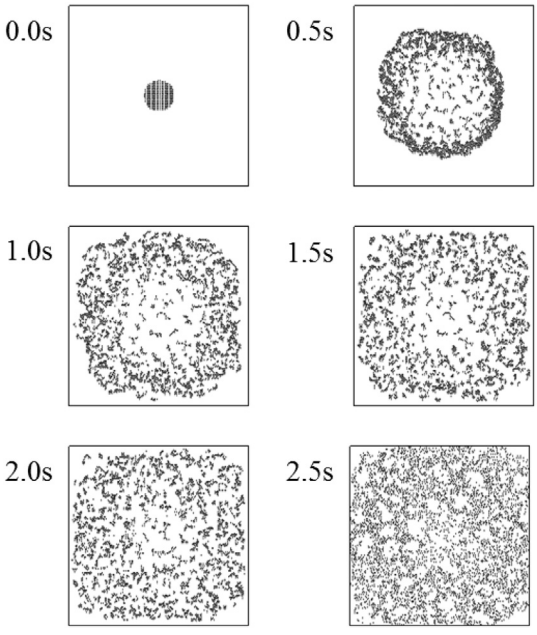

Fig. 6. Time evolution for particle distribution of $k = 4000$ J/m^3 at 85 °C projected onto the horizontal plane.

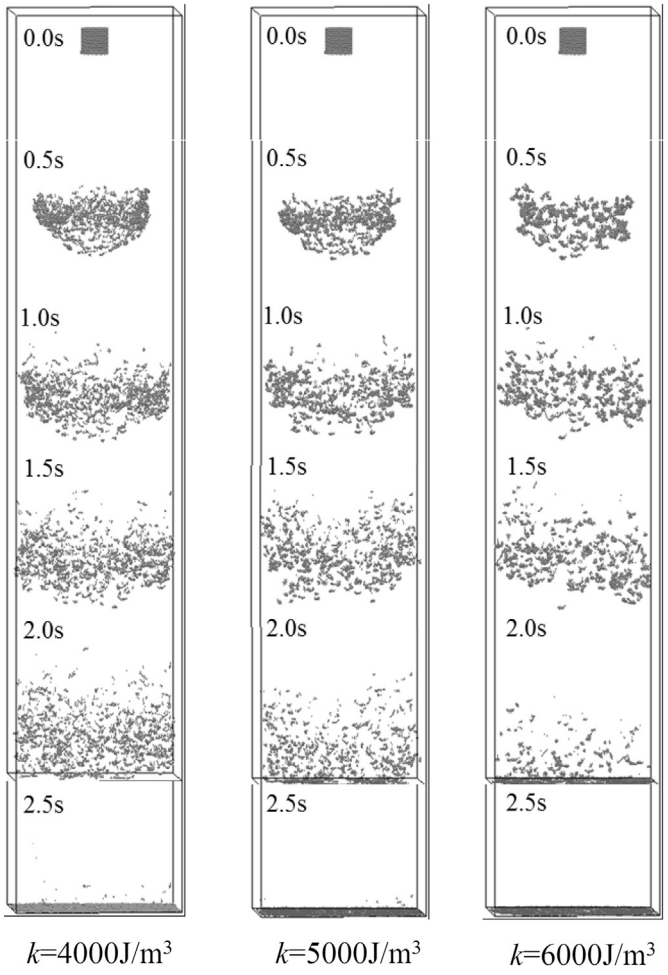

Fig. 7. Time evolution for particle distribution of 85 °C projected onto the vertical plane.

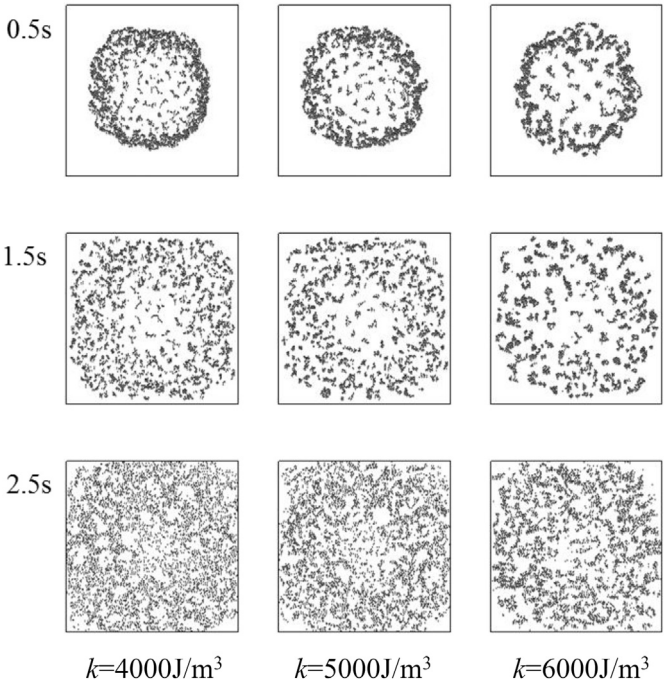

Fig. 8. Time evolution for particle distribution of 85 °C projected onto the horizontal plane.

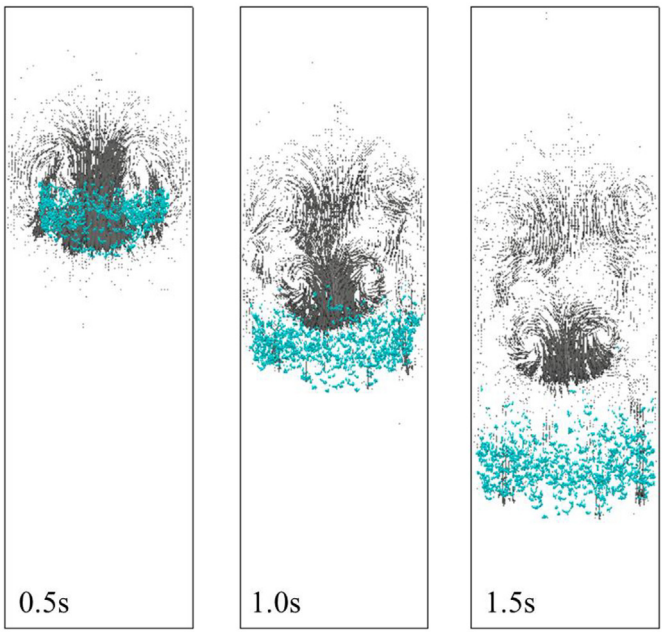

Fig. 9. Time evolution for liquid velocity on the central section and particle distribution ($k = 4000$ J/m^3, 85 °C).

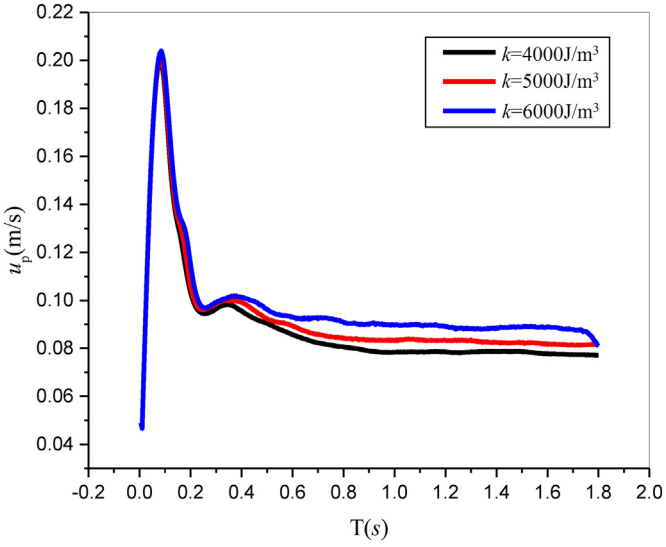

Fig. 11. Time variation for sedimentation velocity of particles of 85 °C.

the time evolution for the particle distribution of three k values, 4000 J/m^3, 5000 J/m^3 and 6000 J/m^3, projected onto the horizontal plane at 85 °C. It is worth mentioning that, when the k value is 6000 J/m^3, all of the particles have fall to the bottom of the bed at 2.5 s, while the k value is 4000 J/m^3, some of the particles are still falling, that is because the particle fall speed will be affected by the cohesive force, as explained later.

The time evolution for the liquid velocity on the vertical plane (x–z plane) passing through the center of the particle-cluster (x = y = 30 mm) is depicted in Fig. 9. The velocity at three time points and the corresponding particle distributions are plotted. When $t = 0.5$ s, a downward liquid flow with higher velocity occurs just above the particle-cluster. The gravitational acceleration, which causes the particles to fall, induces the liquid flow through the drag force acting on the particles. The relative sedimentation of the particles initially arranged in the half upper part shown in Figs. 5 and 6 is due to this downward liquid flow. A pair of large-scale eddies appears around the downward liquid flow. Such organized vertical structure is the wake of the particle-cluster. At $t = 1.0$ s, the developed vortex ringwhirls up the particles, and accordingly it produces the particle distribution of spherical cap type. When $t = 1.5$ s, an liquid flow in the horizontal direction occurs just below the vortex ring, making the particles disperse in the direction. The same phenomenon also has appeared in the gas-solid system [19].

The effect of the change of k value on the fall of the particles has been mentioned above. In the experiment or industrial production, it is difficult to determine the k value through the experimental method directly. There is little research about the k, at the same time; there is no good way to determine the value of k in the literature. In this paper, the results of contrast experiment and simulation are obtained. By using this method, the accurate range of k value can be obtained. Fig. 10 is the

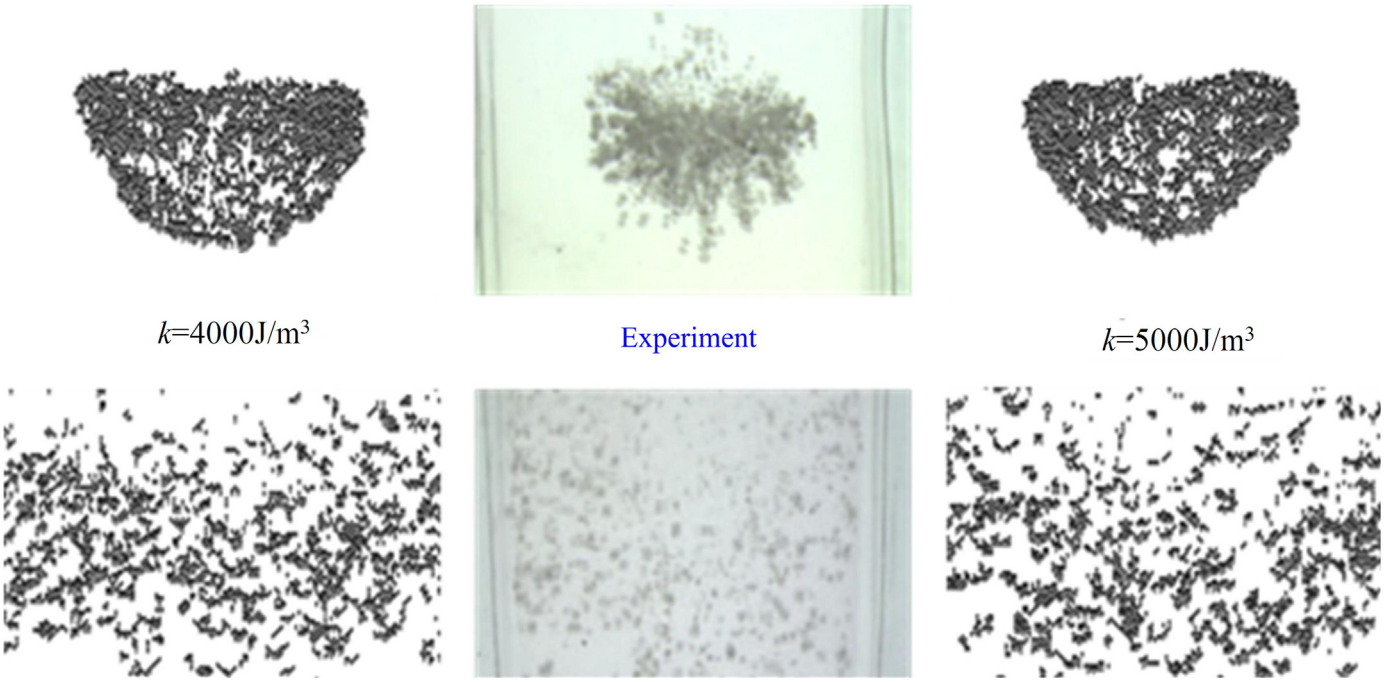

Fig. 10. Comparison of the particle sedimentation process in the experiment and the simulation.

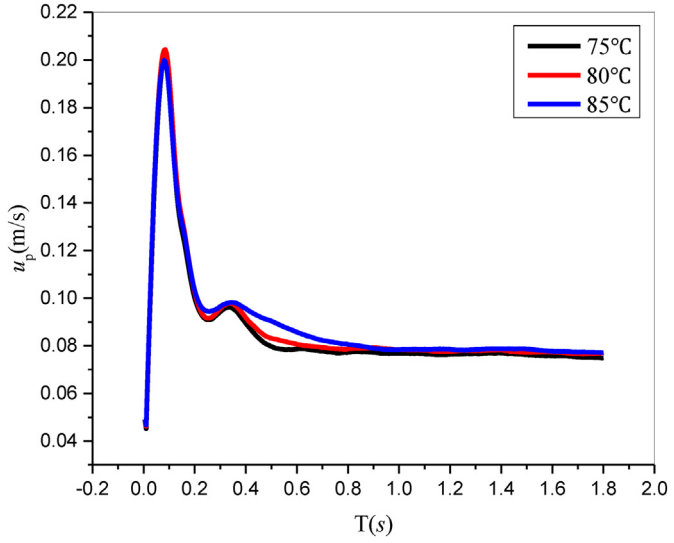

Fig. 12. The comparison of u_p between different temperatures ($k = 4000$ J/m^3).

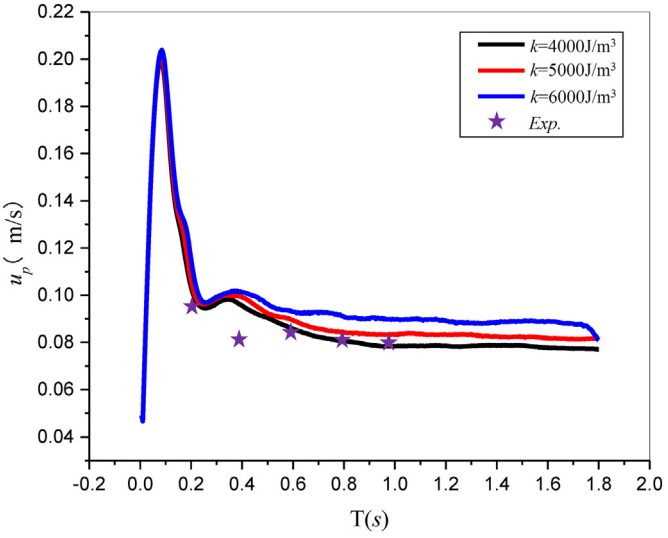

Fig. 13. Comparison of the sedimentation velocity of particles in the experiment and the simulation.

comparison of the particle sedimentation process in the experiment and the simulation results. The experimental results are compared with the simulation results of two k values. When the sedimentation process begins, the shape of the particles in the experiment turns into a hemispherical shape quickly, this process is in agreement with the simulation process. As the particles continue to fall, the hemispherical surface continues to expand and becomes an irregular dispersion. By comparing the size of the particle agglomeration, the range of k value can be judged directly, that is, between 4000 J/m^3 and 5000 J/m^3.

4.2. Time evolution of particle velocity and forces

In the sedimentation of the particles, two quantities are the key of the research, one is the particle velocity, the other is the force between particles. The sedimentation velocity of the center of the blob is shown in Fig. 11 where u_p is the velocity for the center of gravity of the particles. It is observed that the blob accelerates rapidly just after the commencement of the particle fall. This is attributable to the fact that the particles are accelerated by the gravity. In a very short period of time, the velocity can reach a maximum value, followed by a deceleration to a mean value, the terminal velocity u_t.The cause of the deceleration can be inferred from snapshots of the time evolution of the blob as shown in Fig. 5. As the blob descends it deforms from the initial cylinder shape into an oblate spheroid due to the resistance exerted by the fluid. An intrusion develops at the rear stagnation point and the blob subsequently forms into a spherical cap shape. As the blob expands the drag force increases, hence retarding the blob. At later times, the blob disperses uniformly in the form of small aggregation. The tendency of the particles motion in the liquid is similar to that in the gas, but because the density and viscosity of the liquid is larger than that of the gas, the acceleration and deceleration of the particles motion in the liquid is faster [19].

Fig. 12 shows the comparison of the velocity distribution with time between the three temperatures, and the k-value is 4000 J/m^3. The terminal speed will increase rising temperature. However, the change of temperature has little effect on the maximum value of velocity and the terminal velocity u_t.

The problem of particle sedimentation velocity in simulation has been discussed above. The particle will eventually reach a stable final velocity during the fall process. Figs. 7 and 8 show the characteristics of particle sedimentation. The experimental phenomenon also confirmed that there is a clear acceleration process followed by a deceleration process of the particle sedimentation process, and then reach a relatively stable sedimentation process. Because the acceleration and the deceleration process are too quick, difficult to measure, therefore the velocity of the particle is measured when the particles reach the basic steady state. Measurement methods and devices have been introduced in the Section 3.2.2. Table 3 is the experimental value of the fall velocity of particles at 85 °C.

Fig. 11 shows the comparison of the velocity distribution with time between the three k-values at 85 °C. The experimental values are compared with the simulation results, and the comparison results are shown in Fig. 13. When the fall time is 0.2 s, the experimental velocity is 0.095 m/s, and the simulation results of different k values are slightly larger, and the velocity is about 0.105 m/s. When the fall time is 0.8 s, the experimental value is 0.08 m/s, and at the same time, the simulated particles sedimentation velocity of $k = 4000$ J/m^3 is 0.0806 m/s, the velocity values of the experiment and simulation are basically the same. When the sedimentation time is 1 s, the experimental values remain unchanged while the simulated values decrease slightly, when k is 4000 J/m^3, the velocity is 0.0784 m/s, and $k = 5000$ J/m^3, the velocity is 0.0833 m/s. The experimental value is between two values. It shows that the cohesive energy density (k) of the experiment is between 4000 J/m^3 and 5000 J/m^3, which is consistent with the conclusion of the previous section.

Table 3
The average experimental velocity of swollen PE particles u_p.

Time (s)	Velocity (m/s)
0.2	0.095
0.4	0.080
0.6	0.085
0.8	0.080
1.0	0.080

Table 4
Cohesive force, hydrodynamic force and weight of different k-values at three temperatures.

	Cohesive force (μN)			Hydrodynamic force (μN)			Weight of particle (μN)		
	75 °C	80 °C	85 °C	75 °C	80 °C	85 °C	75 °C	80 °C	85 °C
$k = 4000$	2.74	2.74	2.81	0.60	0.63	0.66			
$k = 5000$	6.52	6.69	7.01	0.60	0.63	0.67	0.59	0.62	0.65
$k = 6000$	12.0	12.6	12.9	0.61	0.63	0.68			

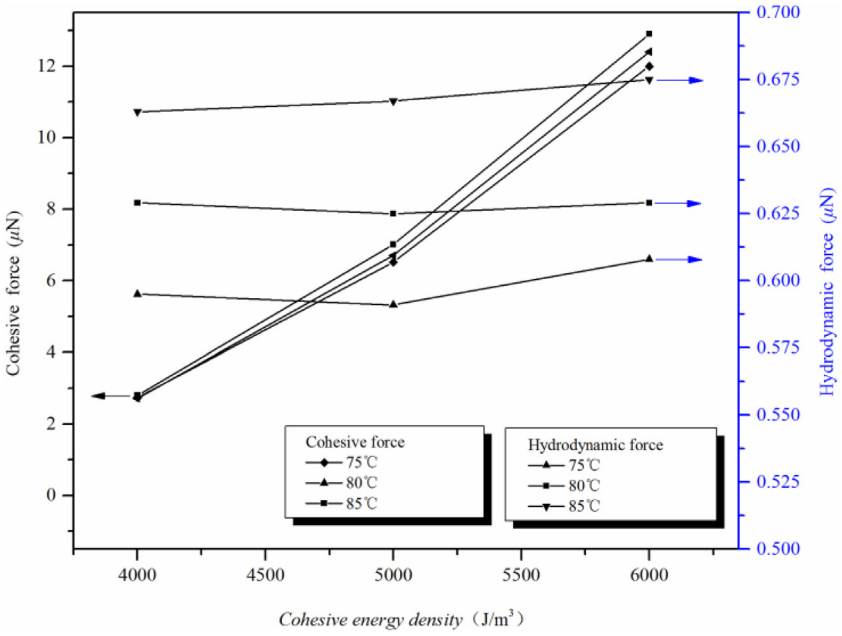

Fig. 14. The comparison of cohesive and hydrodynamic forces between simulation results with different temperatures.

In the sedimentation experiment, the cohesive force between particles and the hydrodynamic force are two typical forces in liquid-solid system. Particles accelerate from rest, followed by a deceleration to a stable value, and the cohesive and hydrodynamic forces also tend to be relatively fixed values. The cohesive and hydrodynamic forces of three *k*-values at three temperatures are calculated and listed in Table 4. Under the same temperature, the cohesive force is advanced with the increase of *k*; and for different temperatures, with the increase of temperature, the cohesive force increases, but the increase rate is less than 10%. For hydrodynamic force, it is not sensitive to the *k* used in SJKR model, but increases with the increase of the temperature. Fig. 14 shows the comparison of cohesive and hydrodynamic forces between simulation results with different temperatures.

Note that in this simulation, there is some correlation between the change of the tendency of hydrodynamic force and sedimentation velocity. We take $k = 4000\ \mathrm{J/m^3}$ (at 85 °C) as an example, Fig. 15 shows the statistics of hydrodynamic force at various moments from 0.01 s and 0.2 s, the trend of the change of hydrodynamic force is consistent with the trend of the change of velocity, which both reach the maximum value at 0.1 s.

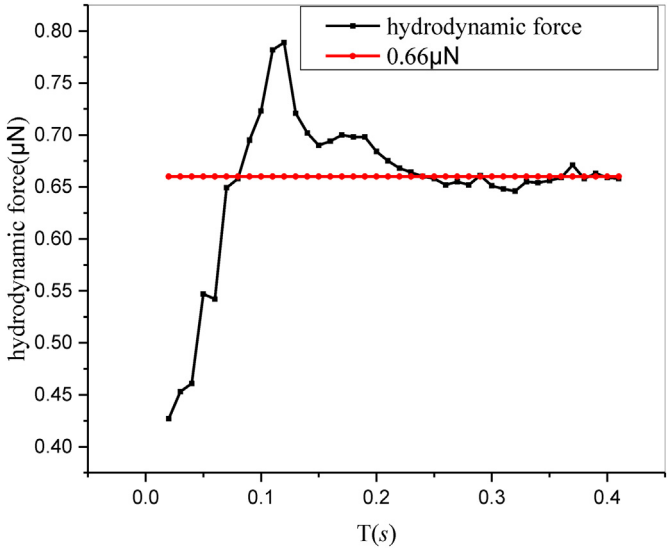

Fig. 15. Time variation for hydrodynamic force of $k = 4000$ at 85 °C.

5. Summary and conclusion

The sedimentation of swollen PE particles was studied via CFD-DEM simulations and experiments, in search of a cohesive energy density measurement. The numerical simulation method is carried out to simulate the sedimentation process of swollen PE particles at three different temperatures. The comparison between experimental results and simulation results is used to measure the surface energy density. This method can also be used in other industrial cases.

In this study, the change of temperature and *k* cause the fluidized state of particles in the fluid. The influence of temperature change is mainly reflected in the cohesive force and hydrodynamic force, and the two forces increase with the increase of temperature. The change of *k* mainly affects the sedimentation velocity, while the influence of hydrodynamic force is small.

Due to limited experimental measurement accuracy, only a range of surface energy density can be given, rather than a more precise number. It is therefore necessary to further study.

Acknowledgement

Financial support from National Natural Science Foundation of China (Grant Nos. 51776212 and 91434113) and National Key R&D Program of China (Grant No. 2018YFB1500902) and Chinese Academy of Sciences (Grant No. QYZDB-SSW-SYS029) and National Key Basic Research Program of China (Grant No. 2015CB251402) are acknowledged. We would like to thank associate Prof. Jianhua Chen for his experimental data and Dr. Xiaoping Qiu for useful discussions to this work.

References

[1] E. Asmussen, A. Peutzfeldt, Surface energy characteristics of adhesive monomers, Dent. Mater. 14 (1) (1998) 21–28.
[2] A. Olah, G.J. Vancso, Characterization of adhesion at solid surfaces: development of an adhesion-testing device, Eur. Polym. J. 41 (12) (2005) 2803–2823.
[3] C.Q. LaMarche, et al., Fluidized-bed measurements of carefully-characterized, mildly-cohesive (Group A) particles, Chem. Eng. J. 300 (2016) 259–271.

[4] K.L. Johnson, K. Kendall, A.D. Roberts, Surface energy and the contact of elastic solids, Proc. Royal Soc. A Math. Physic. Eng. Sci. 324 (1558) (1971) 301–313.
[5] B.V. Derjaguin, V.M. Muller, Y.P. Toporov, Effect of contact deformations on the adhesion of particles, J. Colloid Interface Sci. 53 (2) (1975) 314–326.
[6] J. Israelachvili, Intermolecular and Surface Forces, Academic Press London, London, 1991.
[7] V.M. Muller, V.S. Yushchenko, B.V. Derjaguin, On the influence of molecular forces on the deformation of an elastic sphere and its sticking to a rigid plane, J. Colloid Interface Sci. 77 (1980) 91–101.
[8] Y. Tsuji, T. Kawaguchi, T. Tanaka, Discrete particle simulation of two-dimensional fluidized bed, Powder Technol. 77 (1993) 79–87.
[9] B. Hoomans, et al., Discrete particle simulation of bubble and slug formation in a two-dimensional gas-fluidised bed: a hard-sphere approach, Chem. Eng. Sci. 51 (1996) 99–118.
[10] B.H. Xu, A.B. Yu, Numerical simulation of the gas-solid flow in a fluidized bed by combining discrete particle method with computational fluid dynamics, Chem. Eng. Sci. 52 (1997) 2785–2809.
[11] A. Di Renzo, F.P. Di Maio, Homogeneous and bubbling fluidization regimes in DEM-CFD simulations: hydrodynamic stability of gas and liquid fluidized beds, Chem. Eng. Sci. 62 (1–2) (2007) 116–130.
[12] P.A. Cundall, O.D.L. Strack, A discrete numerical model for granular assemblies, Geotechniques 29 (1979) 47–65.
[13] A. Wachs, et al., Grains3D, a flexible DEM approach for particles of arbitrary convex shape — part I: numerical model and validations, Powder Technol. 224 (2012) 374–389.
[14] Z.Y. Zhou, et al., Discrete particle simulation of particle-fluid flow: model formulations and their applicability, J. Fluid Mech. 661 (2010) 482–510.
[15] Q. Li, V. Rudolph, W. Peukert, London-van der Waals adhesiveness of rough particles, Powder Technol. 161 (3) (2006) 248–255.
[16] Y.I. Robinovich, et al., Adhesion between nanoscale rough surfaces, J. Colloid Interface Sci. 232 (2000) 10–24.
[17] The Liggghts User Manual2019.
[18] J.H. Walther, P. Koumoutsakos, Three-dimensional vortex methods for particle-laden flows with two-way coupling, J. Comput. Phys. 167 (1) (2001) 39–71.
[19] T. Uchiyama, Numerical simulation of particle-laden gas flow by vortex in cell method, Powder Technol. 235 (2013) 376–385.